Applied Water Science (2025) 15:94
https://doi.org/10.1007/s13201-025-02379-4

ORIGINAL ARTICLE

A comparative study on removal of boron via pervaporation and vacuum membrane distillation using zirconium metal–organic framework-loaded poly(lactic acid) membrane

Filiz Uğur Nigiz[1] · Burcu Tan[2] · Tijen Ennil Bektaş[1] · Betül Karakoca[2]

Received: 5 August 2024 / Accepted: 20 January 2025 / Published online: 7 April 2025
© The Author(s) 2025

Abstract

Boron mineral is very important for the life. However, exceeding the standards of boron minerals, especially in water to be used as domestic water, causes health and environmental problems. The commercial method used to separate boron minerals from water is reverse osmosis. In recent years, promising results have been obtained with the membrane distillation (MD) method. However, another method that is as effective as this method is pervaporation (PV). The most important component that affects performance in both methods is the membranes. In this study, zirconium-based metal organic framework (MOF) material was synthesized and added to the polylactic acid (PLA) membrane and boron was removed by pervaporation and membrane distillation methods. While the selective layered asymmetric membrane was prepared for pervaporation, porous membranes were prepared for membrane distillation. The effect of MOF additive on the morphology, mechanical strength, and separation properties of the membrane was investigated. Additionally, the effects of boron concentration and temperature on the separation performance in both methods were examined. As a result, the mechanical strength of membranes with MOF added increased significantly from 2.41 to 8.20 MPa. 99.9% boron removal was achieved in both methods. While the highest flux value was calculated as 8 kg/m^{2}h in pervaporation at 6 ppm boron concentration, it was calculated as 11.33 kg/m^{2}h in membrane distillation.

Keywords Polylactic acid membrane · MIL 140A · Boron removal · Membrane distillation · Pervaporation

List of symbols

Abbreviations

AGMD	Air-gap membrane distillation
DCMD	Direct contact membrane distillation
DMF	N, N-dimethylformamide acid
FTIR	Fourier transform infrared spectroscopy
GO	Graphene oxide
MD	Membrane distillation
MOF	Metal organic framework
PLA	Polylactic acid
PP	Polypropylene
PTFE	Polytetrafluoroethylene
PV	Pervaporation
PVA	Polyvinyl alcohol
PVDF	Polyvinylidene fluoride
PVP	Polyvinylpyrrolidone
RO	Reverse osmosis
SEM	Scanning electron microscopy
SVMD	Sweeping gas membrane distillation
VAGMD	Vacuum-assisted air-gap membrane distillation
VMDC	Vacuum membrane distillation crystallization
VMD	Vacuum membrane distillation
XRD	X-ray diffraction
Zr	Zirconium

Symbols

A	Effective membrane area (cm^2)
C	Concentration of boron (ppm)

✉ Filiz Uğur Nigiz
filiz.ugurr@gmail.com; filiz.ugur@comu.edu.tr

Burcu Tan
burcu.tan88@gmail.com

Tijen Ennil Bektaş
ennilbektas@comu.edu.tr

Betül Karakoca
bet.kar@hotmail.com

[1] Chemical Engineering Department, Çanakkale Onsekiz Mart University, Çanakkale, Turkey

[2] School of Graduate Studies, Çanakkale Onsekiz Mart University, Çanakkale, Turkey

F	Flux (kg/m^2.h)
R	Rejection (%)
t	Operation time (h)

Introduction

Boron is necessary for organisms in all phylogenetic kingdoms to complete the life cycle (with deprivation inhibiting reproduction, where growth, development, or maturation is impaired)(Nielsen 2014). "Paracelsus"—a German-Swiss Renaissance physician, botanist, astrologer, and philosopher—coined this well-known quote about 500 years ago. The adage, "The dose makes the poison" is perhaps the most famous quote in the history of toxicology (Gantenbein 2017). For this reason, when the amount of boron in irrigation water is slightly higher than necessary, it becomes toxic to plants. The concentration of boron minerals, which is important micronutrients in plant growth and development, in irrigation water or soil plays an important role in crop yield (Yapici 2011). The recommended boron content in drinking water according to WHO guidelines was revised to 2.4 mg/L in 2011 (Alharati et al. 2018; Segal et al. 2018). To comply with these legal regulations, desalination, which is the process of purification of seawater and wastewater, is used (Gude 2017).

Traditional desalination methods are thermal technologies based on evaporation of water and collection of condensates. The newest commercial technology for desalination is based on membrane treatment and membrane desalination installations account for close to 80% of all desalination facilities. Desalination by reverse osmosis (RO) dominates current desalination markets. However, RO has some drawbacks: increased driving force is required to handle higher concentration brine. This leads to higher costs. In addition, RO membrane is susceptible to fouling. Moreover, in order to completely remove some substances such as boron, the reverse osmosis system must be applied in several stages. Therefore, innovative membrane technologies are proposed to improve for desalination and boron removal performance (Prihatiningtyas and Van der Bruggen 2020). Pervaporation (PV) stands out among other membrane separation technologies with its low energy cost (Castro-Muñoz et al. 2019a, 2019b). At the same time, although the salinity of the water increases, the separation efficiency does not decrease (Liang et al. 2014). Compared with membrane distillation, pervaporation desalination uses hydrophilic materials to effectively reduce membrane fouling (Kuznetsov et al. 2007). A nonporous, dense polymer membrane is generally used in the pervaporation process. Providing the pressure difference with vacuum, the product selected by the membrane passes to the bottom stream as vapor phase. The purpose of the use of non-porous membranes is to ensure that no pollutants pass through the membrane (Kuznetsov et al. 2007). However, the mass transfer efficiency of the membranes used in PV is relatively low (Liang et al. 2014). Membrane performance is still key in evaluating the effectiveness of pervaporation (Smitha et al. 2004). Existing membranes are prepared from organic polymers, inorganic materials, and their composites. Polymeric membranes still dominate the membrane market (Kang and Cao, 2014; Lipnizki et al., 1999). The most important part of the system is the membrane. Therefore, researches are still focused on the production of suitable and high-performance membranes. Although pervaporation is prominent in the desalination process, very few studies have performed elemental separation. Therefore, the separation performance of many ions in pervaporation has not been explained, yet. There are a limited number of studies on boron removal from model seawater or groundwater by pervaporation. However, flux values in most of them are very low. Ozekmekci et al., have prepared a graphene oxide (GO)/polyvinylpyrrolidone (PVP)/polyvinylidene fluoride (PVDF) hybrid membranes and investigated boron removal from industrial wastewater They reported the highest flux of 0.755 kg/m^{2}h and a boron rejection of 99.86% (Ozekmekci et al. 2021).

Another method used in desalination and boron removal is membrane distillation (MD). There are basically four types of MD configurations: direct contact membrane distillation (DCMD), air-gap membrane distillation (AGMD), vacuum membrane distillation (VMD), and sweeping gas membrane distillation (SGMD). VMD is an attractive and cost-effective membrane technology (Ravi et al. 2020; Najid et al. 2021; Si et al. 2022). According to the principle of VMD, a vacuum is applied to permeate side of a hydrophobic microporous membrane and a phase change occurs prior to separation processes. The mass transfer in this system is in vapor state. The water evaporates at the pore entrance, diffuses across the membrane, and condenses outside the membrane module. The driving force of the process is the partial vapor pressure difference between the side and of the membrane (Mericq et al., 2009). In terms of the separation route, VMD resembles pervaporation. However, the membrane used in VMD is porous and hydrophobic. While the porosity of the membrane used allows higher fluxes compared to pervaporation, low ion rejection values can be obtained in the separation of components that have low kinetic diameter such as boron. Many innovative membrane modules are currently being developed to avoid separation limitations in the MD system (Ali et al. 2024).

In a study performed by Jia et al. (2017), boron removal from radioactive water was performed with a polypropylene (PP) membrane using vacuum membrane distillation crystallization (VMDC). In this study, boron concentration was kept between 0.5 and 100 g/L, temperature between 20 °C and 70 °C, and vacuum pressure between 0.40 and 0.97 atm.

As a result, the highest flux of 6.90 L/m^{2}h and the highest boron rejection of 99% were obtained (Jia et al. 2017). In a study performed by Alkhudhiri et al. (2020), the efficiency of different membrane distillation processes on boron removal was investigated. The boron concentration was between 1.5 and 30 ppm, and the temperature was between 40 °C and 70 °C. In this study, boron was removed from synthetic seawater with polytetrafluoroethylene (PTFE) membrane using VMD. As a result, 5.86 kg/m^{2}h flux and > 99.2% boron rejection were obtained. Among MD technologies, VMD gave the best flux results (Alkhudhiri et al. 2020). In a study performed by Salmanli et al. (2022), boron removal was performed in a synthetic boron solution with commercial membranes of polyvinylidene fluoride (PVDF), PTFE, and PP using vacuum-assisted air-gap membrane distillation (VAGMD). As a result, the highest result was obtained as 29 L/m^{2}h flux and 99.2% of boron rejection with PP membrane (Mutlu Salmanli et al. 2022). In a study performed by Chen et al. (2019), a two-stage membrane process was performed for boron removal from synthetic radioactive wastewater. In the first step, ceramic nanofiltration membrane was used for ion removal. In the second stage, boron removal was carried out with a hydrophobic ceramic membrane using VMD. Boron concentration was between 1 and 107 g/L. As a result, higher than 20 L/m^{2}h flux and 99.9% boron rejection were obtained (Chen et al. 2019).

The primary shortcomings of MD membranes are fouling, wetting, stability, heat and mass transfer, and resistance. Therefore, research efforts should be directed toward developing next-generation membranes that can fully satisfy the requirements for practical saltwater desalination (Gontarek-Castro et al. 2022). The most important feature of the membranes used in MD is hydrophobicity. Incorporation of different additives (CNT, ZIF, etc.) into the membrane eliminates the problem of water wetting by providing hydrophobicity (Vatanpour et al. 2023). Especially in the MD process, porosity is important to eliminate the temperature and concentration polarization. The electrospun membranes have enabled the production of membranes with commercializable potentials due to their tunable pore size and high porosity.

Another problem is the fouling. The deposition of organic and inorganic particles on the membrane structure is defined as membrane fouling. Hydrophilic materials are recognized as the best choice for addressing this problem and minimizing the fouling. Recently, hydrophilic 2D nanomaterials (such as graphene oxide, MXene) are suggested to improve fouling resistance (Castro-Muñoz 2023).

In this study, boron removal was performed comparatively using pervaporation and vacuum membrane distillation. Both methods are advanced membrane separation processes. They have similar and different features to each other. For example, pervaporation is not a thermal separation method, but the temperature is also one of the parameters affecting separation performance, while membrane distillation is classified under the thermal-based process. There is a pressure difference between the sides of the membrane in both methods, and the driving force is the pressure difference.

The role of the membrane in separation is the primary distinction between membrane distillation and pervaporation (Khayet and Matsuura 2004; Ortiz et al. 2001). The vapor–liquid contact is supported by the membrane distillation. The separation occurs in a vapor phase. In pervaporation, evaporation occurs when the liquid phase passes through the membrane. Membranes that are utilized in membrane distillation are hydrophobic and porous. The pervaporation membranes have a non-porous surface. The mass transfer in pervaporation is explained by the solution-diffusion model. The method requires water and membrane material to interact through processes like hydrogen bonding, ion–dipole interactions, and dipole–dipole interactions (Chapman et al. 2008; Liu and Jin 2021). However, in membrane distillation, the membrane and water do not interact as much as possible. Three fundamental mechanisms: Knudsen diffusion, Poiseuille flow (viscous flow), and molecular diffusion control the mass transfer in MD (Drioli et al. 2015; Alkhudhiri et al. 2012). The membrane's porous structure has an impact on the membrane's permeability during membrane distillation. As a result, the membrane's porosity and pore size determine the permeability in MD (Ortiz et al. 2001; Al-Harby et al. 2023; Yadav, et al., 2021a; Yadav, et al., 2021b). Membrane affinity, thickness, nanostructure, and charge density (for a charged membrane) affect membrane permeability in pervaporation (Li et al. 2023; Ortiz et al. 2001; Liu and Jin 2021).

When membranes for MD and PV are manufactured with the same materials, at the same thickness, and carried out under similar operating conditions, membrane distillation produces noticeably larger fluxes than pervaporation (Ortiz et al. 2001). In contrast to membrane distillation, pervaporation has a much higher selectivity. Pervaporation produces lower flux results than membrane distillation; however, depending on the diffusion stage, there is a much larger mechanical mass transfer resistance. As a result, the greater affinity for the target molecule to be transferred to the downstream side is related to higher selectivity in PV (Wang et al. 2016). Especially nowadays, when green chemistry studies are on the rise, the separation technique must also consist of sustainable materials. While bio-based membranes such as alginate and chitosan are used in the PV, the use of fluorinated membranes such as PTFE and PVDF in the MD system limits the sustainability of the system. Therefore, it is important to use biodegradable and biobased membranes in the MD system. In recent years, using of cellulose-based

membranes in MD is promising (Gontarek-Castro and Castro-Muñoz 2024).

In this study, polylactic acid-based membranes with high mechanical strength and high separation performance were prepared and used for desalination via pervaporation and vacuum membrane distillation. Polylactic acid or polylactide (PLA) is a bio-based, biodegradable, biocompatible polymer. It can be obtained from sources such as cornstarch, sugarcane, and other renewable biomass products, or waste (Nofar et al. 2019). In this context, PLA was tested in the desalination study for the first time. To improve the separation performance of the membrane, a metal–organic framework (MOF) was added to the PLA matrix. Metal–organic lattices are microporous materials containing organic and inorganic particles bonded into three-dimensional crystal lattices (Van De Voorde et al. 2015). MOFs can be used as catalysts in catalytic processes, as molecular separators in gas storage, and in many other areas (Yahaya et al. 2020). MOFs have high crystal structures, strong bonding, and high separation properties (Hong et al. 2021; Kalaj et al. 2020; Wu et al. 2020). MOFs have adjustable and designable pore sizes and are therefore used in separation applications. It was also reported that Ag-functionalized MOFs can be effective for the antimicrobial functionality of membranes (Vatanpour et al. 2024).

In this study, porous and asymmetric PLA-MOF nanocomposite membranes were prepared, characterized, and used in pervaporation and membrane desalination systems for boron separation. MIL 140A material, a zirconium-based MOF, was synthesized for this purpose depending on its triangular and narrow cage diameters that prevent the passage of boron elements. In addition, the fact that zirconium-based MOF materials exhibit stable performance in an aqueous environment is the main reason for choosing. Membranes were prepared with the same materials. The membrane used in pervaporation was asymmetric with a non-porous skin layer, while the membrane in membrane distillation was synthesized as porous. The effects of MOF concentration, boron concentration, and temperature on the comparative performance were examined. According to the detailed literature review, PLA-Zr-MOF material has not been used for boron removal before. In addition, the comparison of two techniques for the same conditions was investigated for the first time within the scope of this study.

Materials and methods

Materials

Polylactic acid (PLA) (Nature Works (2003D) was provided.), zirconium chloride ($ZrCl_4$, with 99% purity), acetic acid (with 99% purity), terephthalic acid ($C_8H_6O_4$, with 98% purity), N, N-dimethylformamide acid (DMF, with > 99% purity), chloroform, methanol (> 99% purity), and boric acid (H_3BO_3, with 99.5% purity) were purchased from Merck Chemicals and Aldrich Chemicals, Türkiye.

MIL 140A synthesizing

MIL-140A hydrothermal synthesis was used (Henrique et al. 2020). For the preparation of MIL 140A, 10 mmol of $ZrCl_4$ and 10 mmol terephthalic acid were mixed with 30 mL DMF in a Teflon liner. The liner is placed in an oven at 220 °C and kept for about 15 h. This reactor was then allowed to cool at room temperature. The obtained mixture was washed with methanol and filtrated. After the filtration, the particles were mixed in 50 ml of methanol overnight and filtrated.

Membrane preparation

In the present study, two methods were applied for desalination. For this purpose, two different membrane structures (asymmetric and porous) were prepared with and without MIL 140A particles. Membranes were prepared using the solution-casting technique. A mixture of PLA (wt. 10%), chloroform, and DMF was prepared and stirred under reflux for 5 h at 80 °C. Different amounts of MIL 140A were added to the solution for the nanocomposite membrane. These solutions are "base" solutions for both membrane morphology. Before the polymer casting, the solution was degassed for 24 h at room conditions.

1. For the preparation of the unfilled asymmetric membrane, the base solution was poured into a glass petri dish and dried for ten minutes at 50 °C. The prepared membrane was removed from the glass petri dish and immersed in water to make an asymmetric structure.
2. In order to prepare MIL-140A doped asymmetric membrane, synthesized MIL-140A (wt. 1%, 2%, 3%, 4%) and 10 mL of chloroform were mixed and homogenized with an ultrasonic homogenizer (Bandelin HD4050) for 30 min. Then the particles were added to the base PLA solution and mixed until became homogeneous. The solutions were poured into a glass surface and dried for ten minutes at 50 °C and then taken to a water bath.
3. For the preparation of unfilled and filled porous membrane, the same solutions were prepared, poured onto a glass petri dish, and immersed in a water bath rapidly for ten minutes. These membranes were immersed in water until used.

Characterization

The morphology of the MIL 140A particles and membranes was analyzed using scanning electron microscopy (SEM)

(QUANTA 400F Field Emission). For the cross-sectional view of the membranes, they cracked in liquid nitrogen. The membranes were analyzed under low vacuum after coating with gold.

The structure of MIL 140A was determined using X-ray diffraction (XRD) analysis (PANalytical EMPYREAN device). The test was conducted in the 2θ range of 4−60° with a scan rate of 2°.

Tensile tests were used to determine the mechanical properties of membranes. The tensile tests were conducted using a Universal Testing Machine (ANKARIN). Membranes were divided into 40 × 10 mm strips. The rate at which they were stretched was 10 mm/min.

Fourier Transform Infrared Spectroscopy (FTIR, Perkin Elmer) was used to determine the chemical structure of the membrane. Analysis was done 650–4000 cm^{-1} wavelength.

The porosities (empirical) of the porous membranes were calculated (Eq. 1). For the test, membranes were cut into 1 cm*1 cm pieces. The samples were immersed in distilled water for 24 h, and they were weighed. For each empirical porosity value, the average of three measurements was obtained (Badini Pourazar et al. 2020).

$$Porosity(\%) = \left(\frac{\frac{Ma-Mb}{\rho a}}{\frac{Ma-Mb}{\rho a} + \frac{Mb}{\rho p}} \right) x100 \quad (1)$$

where ρa and ρp are the density of water and PLA polymer, respectively. Ma is the membrane's weight after water uptake, and Mb is the weight of the dry membrane.

Contact angle tests (Dataphysics TBU OCA 11) were applied to all membranes. Measurements were taken from 5 different distances, and their average values were arranged.

Desalination

Pervaporative desalination

For pervaporation tests, the membrane was placed in the membrane cell and the membrane cell was placed in an oven to supply the desired temperature. The feeding part (upstream side) of this cell is kept at atmospheric pressure, while the downstream side is connected to a vacuum pump. Cold traps with liquid nitrogen were equipped to condense the water vapor after desalination. The downstream pressure was kept constant at 10 mbar. All experiments were performed for four hours with 250 mL of feed solution. The effective membrane area was about 9.26 cm^2. A basic representation of PV is shown in Fig. 1.

In the first part, the temperature (50°) and the feed boron concentration (10 ppm) were kept constant to determine the membrane that gave the highest boron removal and flux results. The pervaporative desalination experiment was performed by placing the unfilled and filled PLA membranes in the membrane cell, respectively. Then the effect of temperature (40, 50, 60, 70 °C) and the feed boron concentration (6, 8, 10, 100, 200, 400, 500 ppm) on separation performance was examined in the pervaporation system.

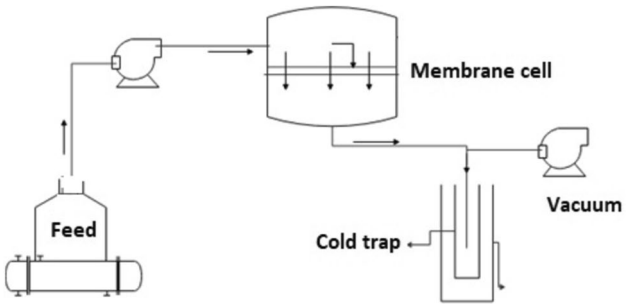

Fig. 1 Pervaporation test unit

The performance of the desalination was evaluated as a function of flux (Eq. 2) and boron rejection (Eq. 3).

where F (kg/m^2h) is the flux, R (%) is the boron rejection, M is the weight of the permeated substance, A is the membrane area, and t is the time, C_f and C_p are the feed and permeate boron concentration, respectively.

$$F = \frac{M}{A.t} \quad (2)$$

$$R = \left(\frac{Cf - Cp}{Cf} \right) * 100 \quad (3)$$

Membrane distillation

A similar experimental system has also been established for the membrane distillation. The membrane was placed in the membrane cell for membrane distillation. In the case of this process, water vapor is connected to the membrane. The membrane cell was kept on the heater to keep the temperature constant. The feeding part of this cell is connected to the feeding tank with the pump, and the outlet part is connected to the trap with the vacuum pump. The experiment was carried out with 250 mL of feed solution. The vacuum pressure was kept constant (10 mbar) in all experiments. The trap was kept in an ice container. The flux and boron rejection results obtained from the experiments for pervaporation and membrane distillation were compared.

Figure 2 shows the experimental systems of membrane distillation.

Two systems are operated in the same conditions with similar membrane materials having different morphology. The difference between these two test systems is the condensation liquid. While liquid nitrogen was used in PV, ice

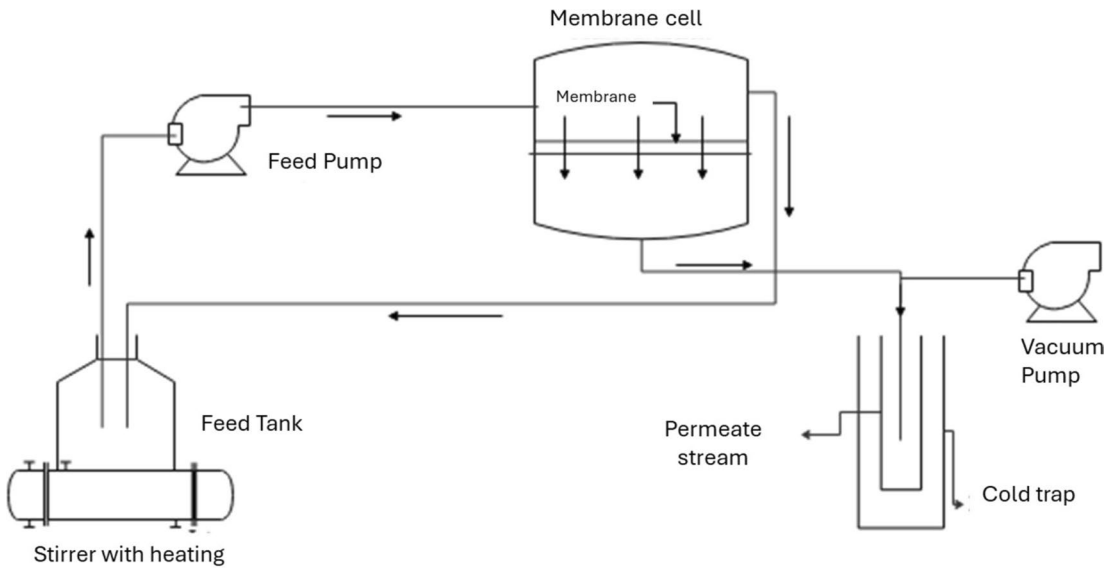

Fig. 2 Acuum membrane distillation test unit

water was used for MD. Since the membrane used in MD is porous, flux can be collected at mild downstream conditions. This significantly reduces the system cost. Additionally, the membrane cell was designed with recycle flow in the membrane distillation process.

Analysis

Boron analyses were done according to the Carmine method (Sarkar et al. 2014) by using a HACH DR 1900 Spectrophotometer device. In this analysis, 75 mL of sulfuric acid and boron reagent kits (Hach, Powder Pillows) was mixed in a flask until dissolved. The prepared solution was divided into two equal volumes (35 mL), one for the blank and the other for the sample containing boron. Two milliliters of distilled water was added to the blank sample, and 2 mL of the boron-containing sample was added to the other solution and was mixed. Then, samples were analyzed with a wavelength of 585 nm.

Results and discussion

Characterization results

In this study, MIL-140A was synthesized and incorporated into the structure of PLA-based membranes. Characterization tests of this material and membranes were carried out. Prepared membranes were used for boron removal by membrane distillation and pervaporation. Figure 3 shows the SEM results of the MIL 140A particles, asymmetric, and porous membranes.

Figure 3a shows the non-porous (top side) and porous (bottom side) structure of the unfilled membrane. The thickness of the membrane was about 60 µm, and the top side was non-porous. The non-porous structure was about 5 µm. Figure 3b shows the MIL 140A loaded asymmetric membrane with the non-porous bottom side. The higher magnification of the micrograph is seen in Fig. 3c. The particles can be clearly seen in this micrograph.

Figure 3d, e, f shows the different magnifications of MIL-loaded porous membranes. The pores are visible in the PLA-based porous membrane. They compared these pores with sponges in their literature studies (Zhou et al. 2019; Tooma et al. 2015; Chen et al. 2014). These porous membranes have microcavities. The different morphology can be clearly seen because of the drying time. In all micrographs, homogeneous pore size, pore distribution, and particle dispersion can be clearly seen. The crystal structure of this material and its homogeneous distribution in the membrane are important to increase MD and PV performance.

In Fig. 4, XRD graph of MIL140A material is given.

In this graph, it is seen that the synthesized MOF material has high crystallinity. In addition, it has been observed that it is fully compatible with the XRD results given for the MIL-140A material synthesized in the literature (Guillerm et al. 2012; Liang et al. 2013).

Figure 5 shows the mechanical analysis results of the asymmetric membrane used in PV and the porous membrane used in MD.

As seen in the figure, MOF addition significantly increased the membrane strength. In particular, there is an increase up to 3 wt.% concentration. When the MOF ratio increased from 0 to 3 wt.%, the tensile stress of

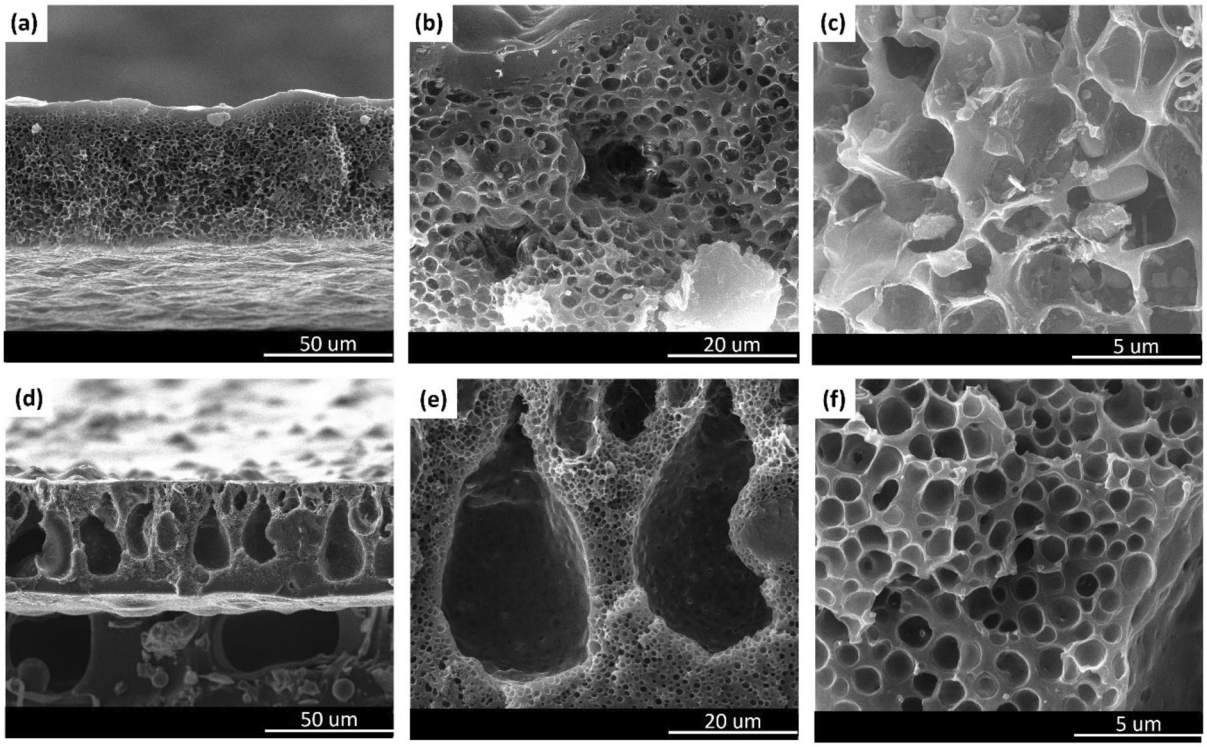

Fig. 3 Cross-sectional SEM micrographs of asymmetric unfilled (**a**), asymmetric 3 wt.% MIL 140A loaded (**b**, **c**), and porous 3 wt.% MIL 140A loaded membrane (**d**, **e**, **f**)

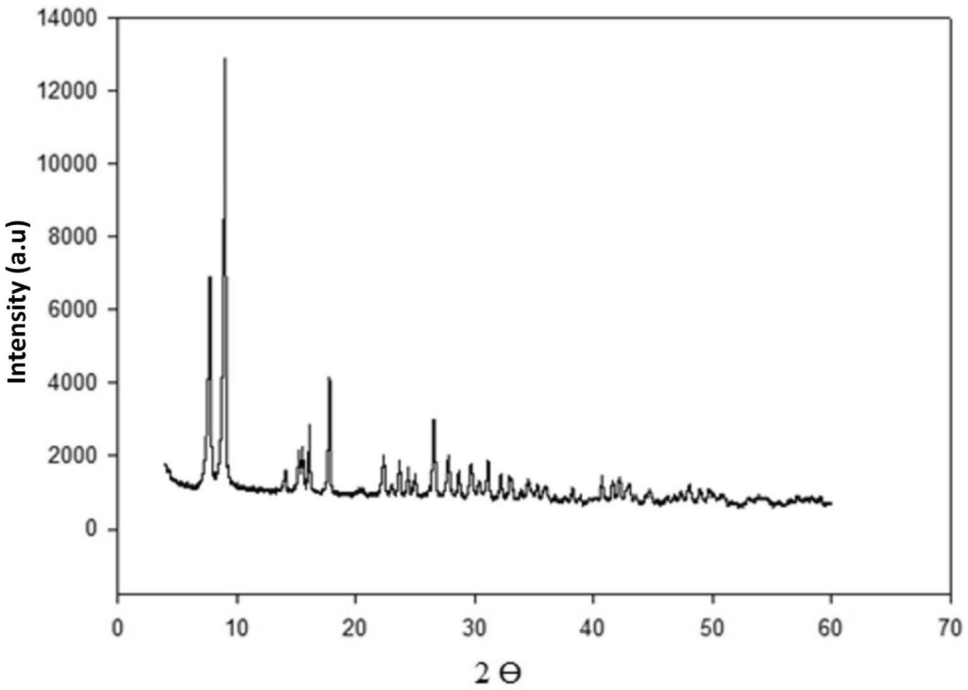

Fig. 4 XRD pattern of MIL 140A

the PV membrane increased from 2.41 to 8.20 MPa. In the MD membrane, an increase was observed from 1.96 to 5.20 MPa. This is due to the high strength of MOF materials. Since the particles are distributed homogeneously within the membrane and the load transfer is distributed homogeneously, the strength increases. A slight

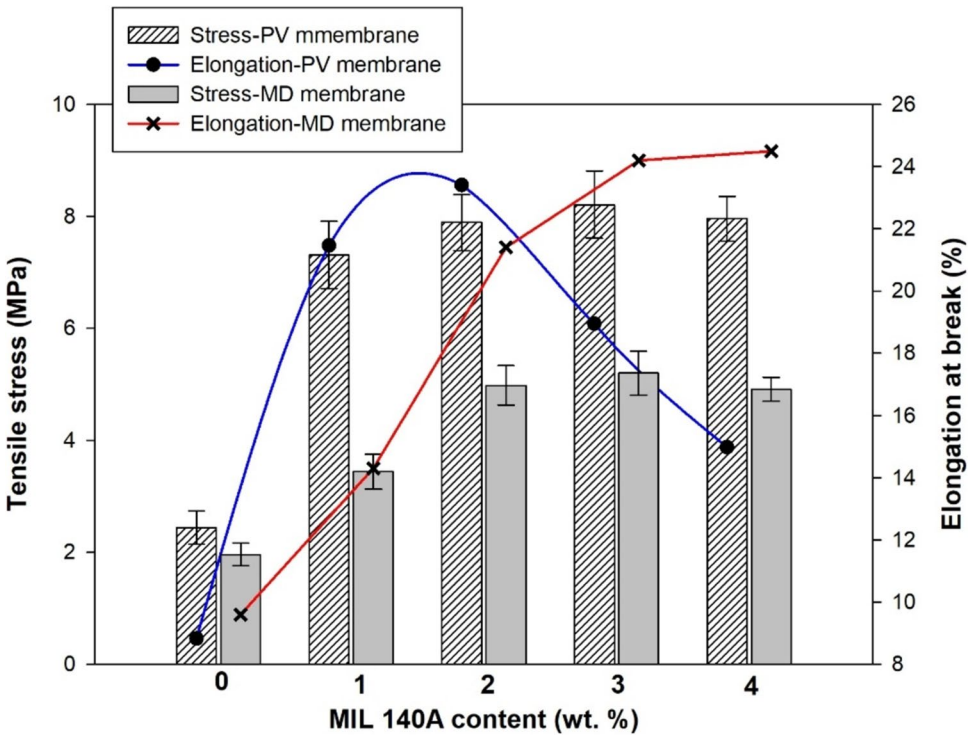

Fig. 5 Mechanical test results of the PV and MD membranes

decrease in 4 wt.% MOF-loaded membrane was observed. This can be attributed to MOF agglomeration. Similar results were also seen in our previous studies. As expected, the strength of non-porous membranes is higher than those of porous membranes. However, the fact that there is not a very high difference showing that porous membranes can also have high strength under pressure. Another finding seen in the figure is that the elongation at break constantly increases in the porous membrane and the flexibility of the membrane increases. In the non-porous membrane, a decrease was observed after 2 wt.% loading.

FTIR analysis was performed for all membranes. Figure 6 indicates the FTIR results of the unfilled and filled membrane.

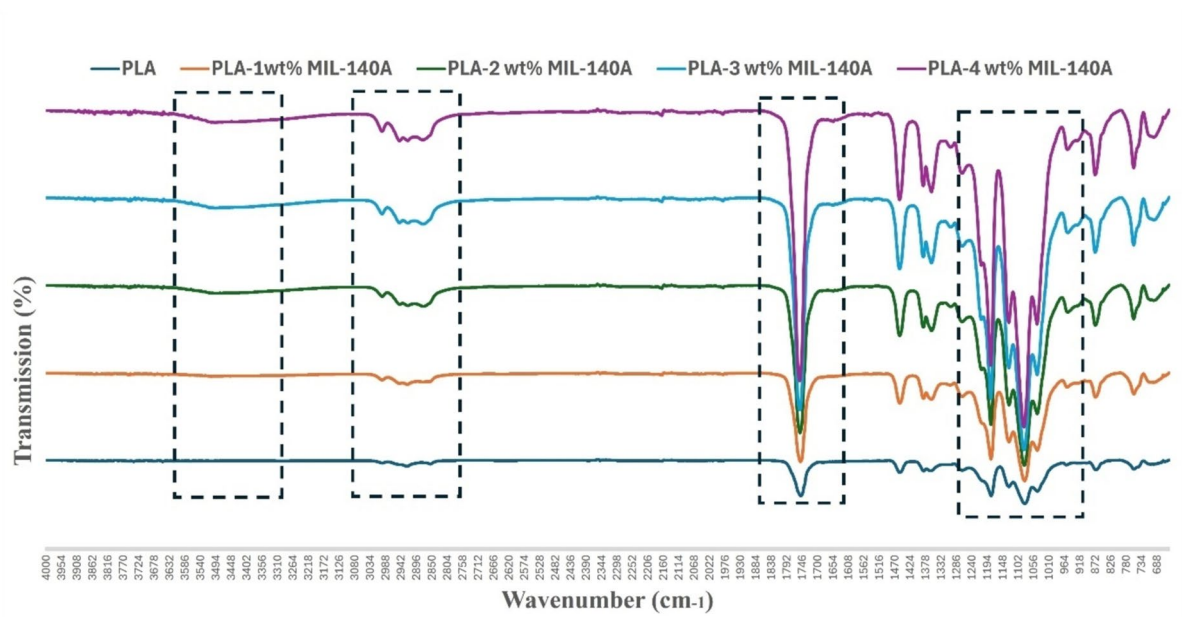

Fig. 6 FTIR spectra of unfilled and filled membranes

The stretching vibration in 3470 cm^{-1} is attributed to O–H banding in nanocomposite membrane. Even though the plain PLA's spectra do not contain hydroxyl groups, the O–H band's intensity rises with MIL 140A incorporation. This is entirely due to the capacity of MOF particles to absorb water. The typical stretching vibration peaks of PLA, corresponding to the asymmetric and symmetric $–CH_3$ groups, are located around 2990 and 2880 cm^{-1}, respectively. Due to the free protonated linker within the pore of MIL 140A, the intensity of C = O bond stretches at 1750 cm^{-1} increases (Butova et al. 2020; Nigiz and Karakoca 2023). The sharp peaks at 1070 cm^{-1} that rise with MIL 140A incorporation are attributed to the Zr–O vibration.

The critical factor for membrane distillation technique is that the membranes should be hydrophobic and porous. Therefore, the surface property and porosity of porous membranes were determined by contact angle test and porosity test, respectively. Figure 7 shows both values as a function of the MIL 140A content. The decrease in the contact angle is due to either the increase in the surface hydrophilicity of the membrane or the increase in the penetration surface area of the water. The increase in porosity increases the penetration area. As can be seen in the figure, the contact angle of the surface with water decreased as MIL 140A content increased. However, this decrease is very small. Therefore, the reason for the decrement is attributed to porosity rather than hydrophilicity as illustrated in the figure. The enhanced porosity may be attributed to the enlarging of the pore size depending on the microsize MIL material. Moreover, it was previously reported that the filler-incorporated membranes have a more porous structure depending on the phase inversion process (Geleta et al. 2023; Holda and Vankelecom, 2015). During the phase inversion, evaporation starts primarily at the interface of the polymer and filler; therefore, the pore size, distribution, and porosity of the composite membranes may be higher than those of the plain membranes.

Boron removal performance of pervaporation and membrane distillation

PLA-based membranes are prepared as porous and asymmetrically. The asymmetric membranes were used in pervaporation, and porous prepared membranes were used in membrane distillation. Since it was aimed to compare pervaporation and vacuum membrane distillation, the experiments were carried out under the same conditions in both methods. Figure 8a indicates the flux results of the

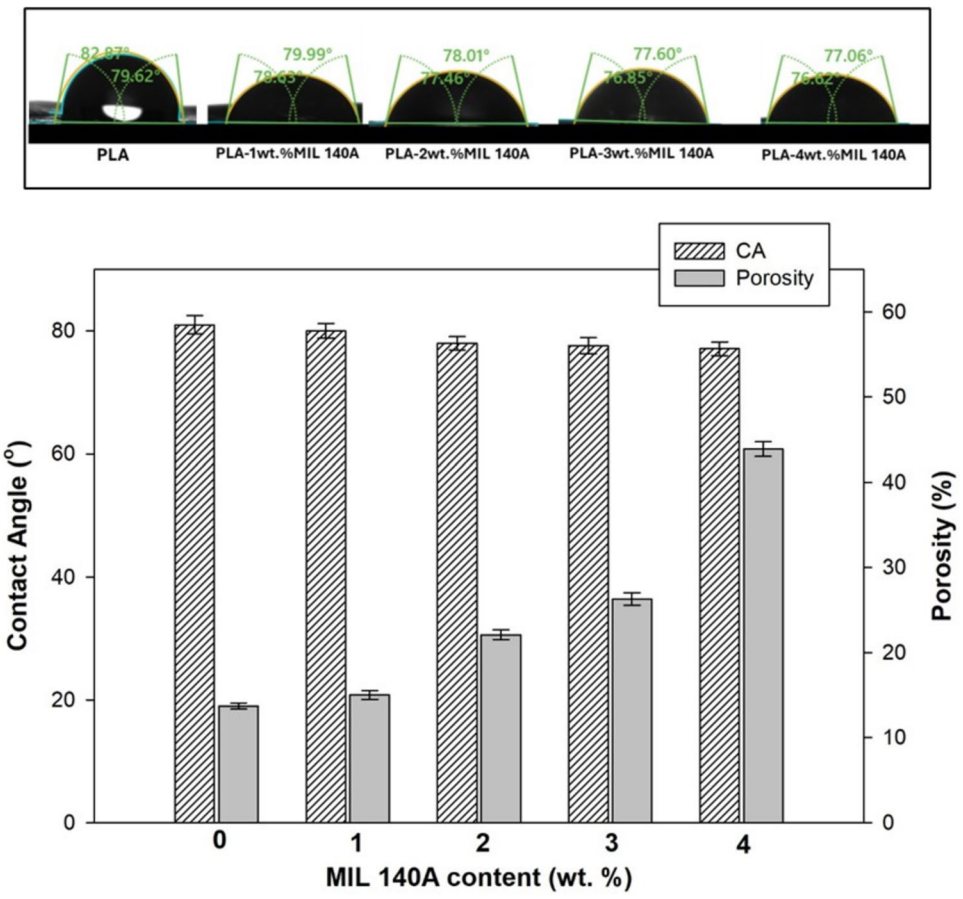

Fig. 7 Effect of MIL 140A on contact angle and porosity

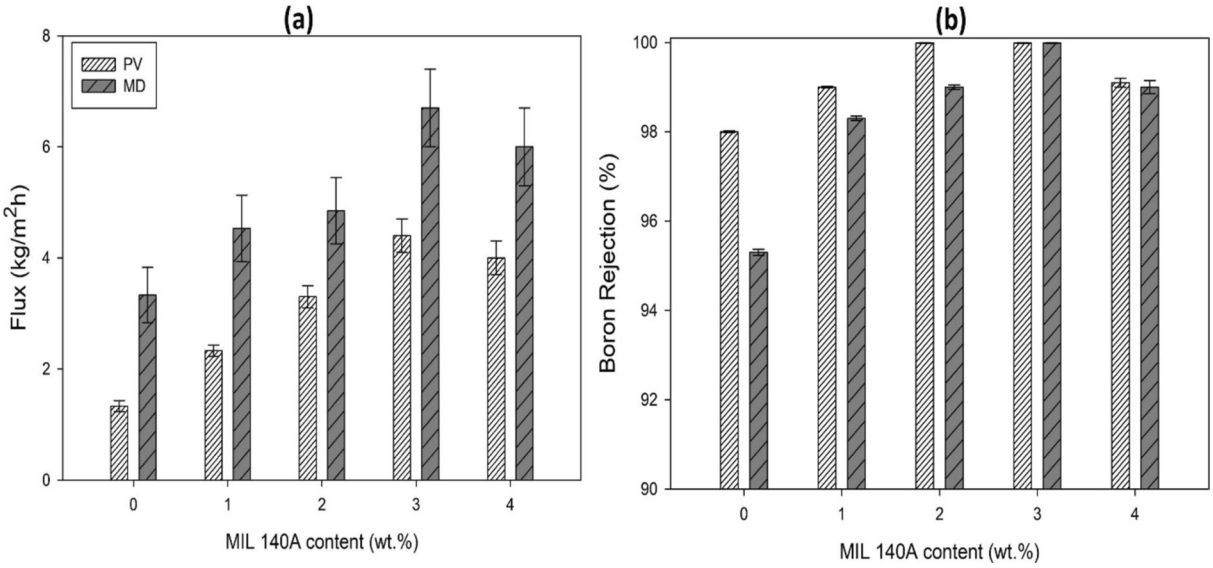

Fig. 8 Effect of MIL 140A ratio on flux (**a**) and boron rejection (**b**) (50 °C temperature and 10 ppm boron)

experiments. As seen in the figure, MIL 140A addition and increasing amount of particles significantly improve the flux in both systems. This increment may be related to the changing crystallinity and glassy transition temperature of membranes. As the crystalline and glass transition temperature decreases, the mobility of the polymeric chain increases, thus enlarging the transition areas of water vapor and increasing the flux value. In our previous study, it was reported that the addition of MIL 140 A causes significant alterations in membrane structure. The melting enthalpy of the membrane decreases substantially from 38 to 25.5 J/g, even though its melting point remains unchanged. The addition of MIL 140 A decreased the membrane's crystallinity depending on the weakened chain bonding. It was also reported that the T_g, temperature of the plain membrane, is higher (59 °C) than nanocomposite (56 °C) (Nigiz and Karakoca 2023). These results were attributed to the decrease in hydrogen bond barrier effect (Xue et al. 2020).

The 3 wt.% MIL-140A doped nanocomposite membrane gave the highest flux result in both methods. The flux of this membrane was calculated as 6.7 kg/m^{2}h for vacuum membrane distillation and 4.4 kg/m^{2}h for pervaporation. MD flux results were higher than that of PV flux results in all membranes due to the porous structure which facilitates the passage of water.

The rejection results are given in Fig. 8b. Similar to the flux results, the rejection results are also improved by the MIL 140A addition. In both methods, 3% MIL-140A doped PLA membrane gave the highest boron rejection result compared to other membranes. In this membrane, boron rejection in MD and PV was calculated as 99.99%. The rejection results of 4 wt.% MIL-140A filled PLA membrane slightly decrease. The decrease should be attributed to the polymer-particle void results in the overlapping of the particles. According to the separation result, the highest separation results were obtained by using 3 wt.% MIL-140A loaded membrane. Hence, the effect of temperature and boron concentration on desalination performance was carried out with this membrane.

Figure 9 shows the separation performance of 3 wt.% of MIL 140A loaded membrane in terms of the varying temperature.

Figure 9a shows the temperature-dependent flux of 3% MIL-140 doped PLA membrane as a result of MD and PV processes. It was observed that the flux increased as the temperature increased in PV and MD. In both methods, the lowest flux values were calculated at 40 °C. The highest flux values were calculated as 6 kg/m^{2}h in PV and 10.41 kg/m^{2}h in MD at 70 °C. The temperature is very important factor in changing the separation performance of PV and MD. The increasing temperature increases the partial pressure of water. Both processes are partially pressure-driven, and flux enhancement is an expected result. Another factor enhancing the flux is the increasing diffusion rate. The water diffusion rate increases with temperature rising in both processes. The temperature is also effective on the structure of the polymer. It is known that the polymer mobility increases and void spaces change with increasing temperature. This enhancement positively affected the flux. However, this mobility change can show a trade-off trend between flux and rejection. So, the rejection values should also be considered when the performance of the membrane is evaluated.

Figure 9b shows the boron rejection results of the nanocomposite membrane. According to this graph, boron

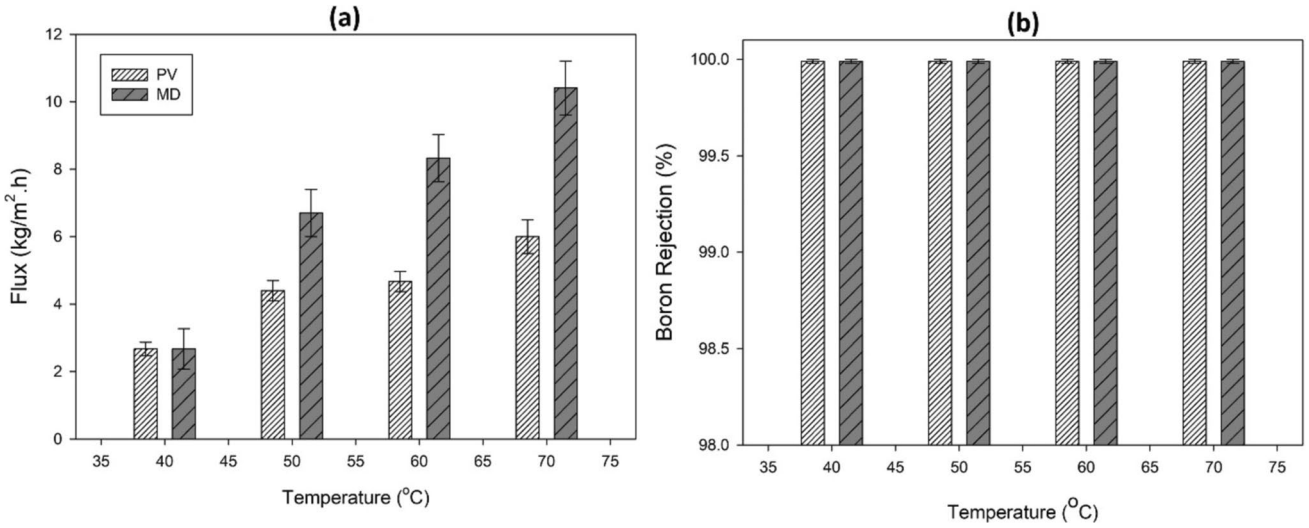

Fig. 9 Effect of temperature on flux (**a**) and boron rejection (**b**) (10 ppm)

rejection was calculated as 99.99% in both methods. Accordingly, although flux values were observed to change depending on the pervaporation and membrane distillation temperature, almost 100% of rejections were calculated. In addition, although the membranes used in membrane distillation were porous, boron rejection did not affect the results.

Figure 10a shows that the highest flux values are calculated at low boron concentration.

While the highest flux value was calculated as 8 kg/m^{2}h in pervaporation at 6 ppm boron concentration, it was calculated as 11.33 kg/m^{2}h in membrane distillation. As the boron ratio in the feed solution increased, the water flow decreased. The decrease in flux may be due to several reasons. First, as the boron concentration in the feed solution increased, the thermodynamic activity of the water and its vapor pressure decreased (Wang et al. 2016). Thus, since the pressure difference between the two sides of the membrane decreases, the flux decreases. Secondly, according to Fick's law, the driving force decreases due to the decrease in the mole fraction of the water (Ünügül and Nigiz 2022). In Fig. 9b, boron rejection results according to boron concentrations are given. All boron rejection results in pervaporation and membrane distillation processes were calculated as 99.99%. The reason for this is that the kinetic diameter of the boron molecule (> 0.85 nm) is larger than that of water (0.28 nm). The high selectivity of the prepared membranes and the kinetic diameter of MIL 140A being smaller than boron brought all the separation results closer to 100%. No boron element was

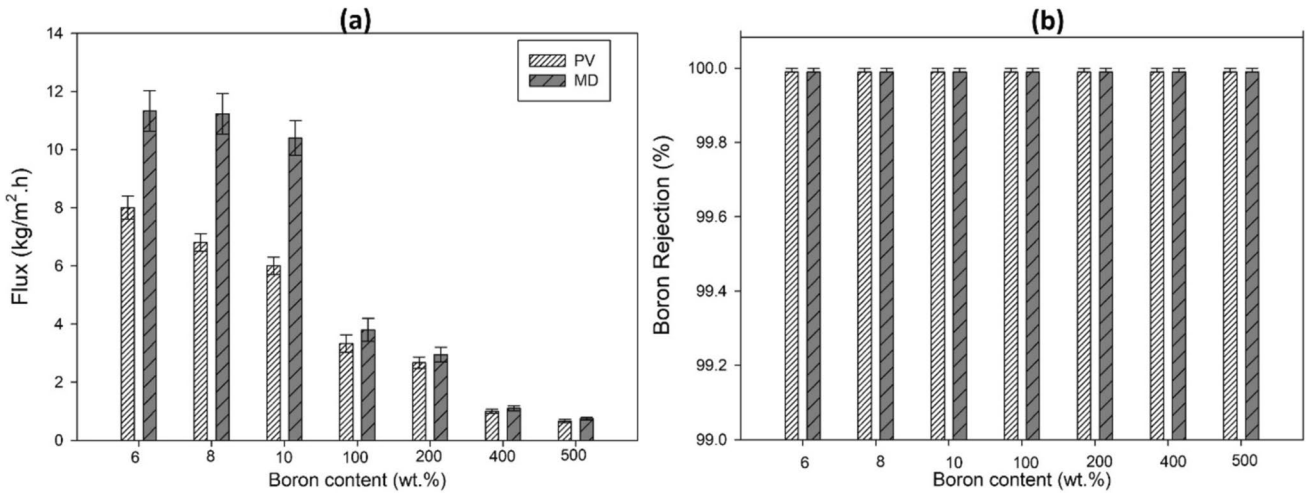

Fig. 10 Effect of boron concentration on flux (**a**) and boron rejection (**b**) (70 °C)

detected in the permeate side in the repeated experiments. As seen in the graph, the increase in boron concentration in the feed solution did not affect the boron rejection. Similar results have been obtained in the literature. Alkhudhiri et al. (2020) reported that the boron rejection results at different boron concentrations. They examined a membrane distillation process and found that although the boron concentration changes, greater than 99.4% boron rejection was obtained (Alkhudhiri et al. 2020). Özekmekçi et al. (2021) performed boron removal using the pervaporation method. In this study, boron rejection results vary between 98.19 and 99.38%, even if the boron concentration changes (Ozekmekci et al. 2021).

Comparison and long-term stability of membranes

There are studies in the literature on boron removal by membrane distillation. However, most of these used commercial membranes, PVDF and PTFE. When the techniques were compared among themselves, it was seen that higher flux results were obtained with vacuum-assisted membrane distillation. The separation percentage varies. Table 1 shows examples of literature studies. The boron removal percentage obtained in this study is quite high, and the flux values are moderate compared to the literature.

In contrast to the MD technique, there is only one study in the literature where the PV technique was used for boron separation. In a study performed by Ozekmekci et al. (2021), PVP/PVDF membrane was used in the PV system at room temperature and 0.755 kg/m^{2}h flux and 99.86% boron rejection were achieved. In our study, the flux value was obtained as 8 kg/m^{2}h with the boron rejection of 99.99%. Therefore, it is seen that the PLA asymmetric membrane is quite selective and has high flux in boron removal application in the PV technique.

The most important factor affecting flux and separation performance in both membrane distillation and PV techniques is membrane fouling. Membrane fouling shows itself as the collection of particles in the water on the surface or in the pores and biofouling due to bacteria and fungi on the surface (Woo et al. 2018; Gryta 2005; Abdel-Karim et al. 2021). Since a porous membrane is used in the MD process unlike PV, wetting is also the biggest cause of fouling in this method. Since vapor passage is involved in both methods, in-pore fouling is usually not seen much. Fouling manifests itself as a decrease in flux. Therefore, the existence of these effects in long-term experiments is discussed.

In this study, 3 wt.% MIL 140A doped PLA membranes were tested for long-term operation. Each set of experiments was used for 6 h, and 12 sets of experiments were performed. Membranes were used in each test without cleaning. While the boron separation performance remained constant above 99%, there was a change in the membrane flux as seen in Fig. 11. This change is less than 7% in the PV membrane (from 4.4 to 4.11 kg/m^{2}h). Because there is only boron in the water used and there is no transition because the membrane surface is dense. However, in the MD technique, the decrease is greater than 12% (from 6.7 to 5.9 kg/m^{2}h). The reason for this was attributed to pore wetting. Because the surface hydrophobicity of the composite PLA is low, this shows that water retention occurs in the pores.

In order to ensure the long-term use of the membrane, either pre-treatment or membrane cleaning at regular intervals is required. Methods such as adsorption, defoaming, coagulation, and oxidation can be given as examples of pre-treatment processes. The basic techniques applied for fouling (accumulation, water retention, and biofouling on the surface) that will prevent membrane flux are known as chemical cleaning, pure water backwashing, drying, aeration, and vibration (Abdel-Karim et al. 2021). In this study, the long-term operating test was also applied with cleaning before each test. Both backwashing and air oven drying (60 °C for 12 h) techniques were applied, and the membranes were cleaned and reused in each set. It was observed that the flux remained almost constant in both techniques. The boron rejection was still above 99.9%, and the flux decrement was obtained lower than 2% for PV and 5% for MD.

Table 1 Comparison with literature studies

Membrane	Technique	Flux	Rejection	References
rGO/PVDF	AGMD	19.2	96.89	Eryildiz, et al., 2021a
PVDF/PTFE	AGMD	27.2	98.5	Ozbey-Unal et al. 2020
PP/PTFE(0.2)	AGMD	> 15	99	Eryildiz, et al., 2021b
PP	DCMD	19,5	99,97	Wen et al. 2016
PP	VMDC	6.9	99.9	Jia et al. 2017
PVDF	VAGMD	20.44	99.5	Mutlu-Salmanli et al. 2023
Commercial	DCMD	14	48	Tan et al. 2021
Commercial	DCMD	N.A	75	Tan et al. 2024
PTFE	VMD	3.21	99.2	Alkhudhiri et al. 2020
PVDF	DCMD	10.55	90.52	Boubakri et al. 2015
PLA-MIL 140A	VMD	11.33	99.99	This study

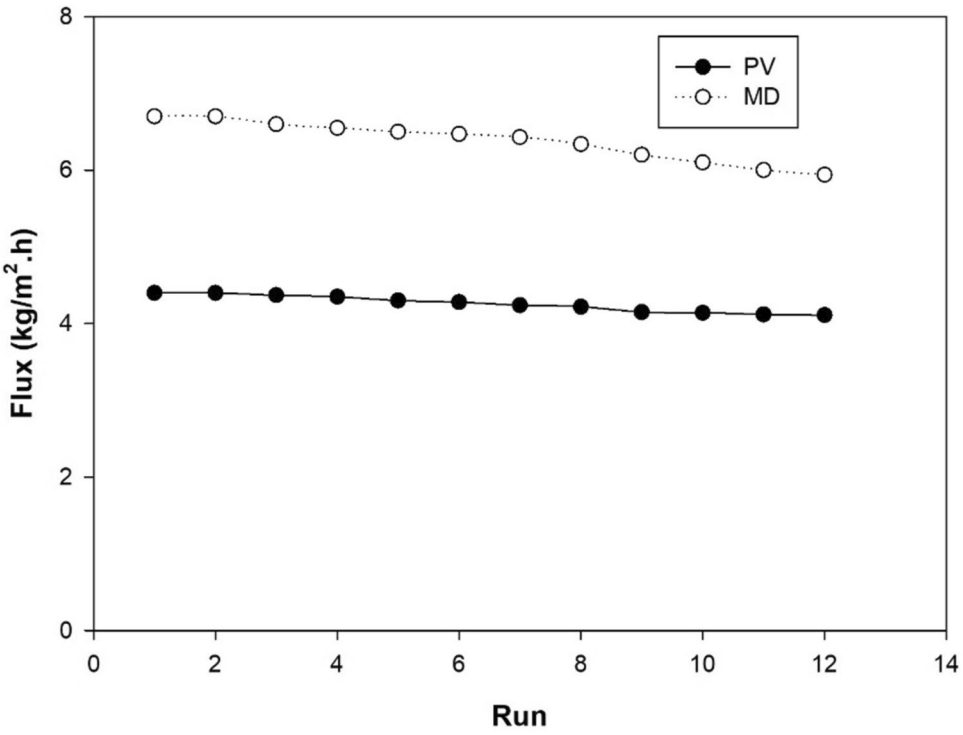

Fig. 11 Long-cycle test for PV and MD (50 °C temperature and 10 ppm boron)

Conclusions

In this work, boron was separated from the simulated water using membrane distillation and pervaporation techniques. MIL 140A was synthesized and incorporated into the PLA membrane to enhance both the physicochemical and separation performance of the membrane. It was observed that MIL particles were distributed homogeneously on the surface and structure of the membrane. According to the mechanical analysis results, especially as the MOF contribution increased from 0 to 3 wt.%, the mechanical strength gradually increased from 2.41 to 8.20 MPa in the PV membrane and from 1.96 to 5.20 MPa in the MD membrane. It was observed that the strength decreased at a higher loading rate. MIL additive significantly increased the separation performance in both methods. While flux values increased with increasing temperature, boron rejection did not decrease. This shows that the trade-off trend occurring in the membrane process has been prevented. While the boron concentration in the feed did not affect the boron rejection, the flux values increased as the boron concentration decreased. The highest flux value in membrane distillation was obtained as 11.33 kg/m^{2}h, whereas the flux was found to be 8 kg/m^{2}h in pervaporation at 70 °C with the feed boron concentration of 6 ppm. Boron rejection was obtained as 99.9% at different boron concentrations, and this result shows that both techniques have high performance in different feed waters (groundwater, seawater, etc.). The boron removal percentage obtained in this study is quite high, and the flux values are moderate compared to the literature. The results of this study also showed that the flux drop was high due to pore wetting in the MD technique in long-term tests and this is probably due to the low hydrophobicity of the membrane. In future studies, MOF and PLA material will be produced as electrospun membranes to increase both hydrophobicity and porosity. Experiments will also be carried out with real seawater and groundwater to examine the commercial use of the membranes.

Funding Çanakkale Onsekiz Mart Üniversitesi, FHD-2022-3900, Filiz Ugur Nigiz, Türkiye Bilimsel ve Teknolojik Araştırma Kurumu, 121Y080, Filiz Ugur Nigiz.

Declarations

Conflict of interest The authors declare there is no financial interests/personal relationships as potential conflict of interest.

Ethical approval There are no human or animal subjects in this article and ethical approvement is not applicable.

Open Access This article is licensed under a Creative Commons Attribution-NonCommercial-NoDerivatives 4.0 International License, which permits any non-commercial use, sharing, distribution and reproduction in any medium or format, as long as you give appropriate credit to the original author(s) and the source, provide a link to the Creative Commons licence, and indicate if you modified the licensed material. You do not have permission under this licence to share adapted material derived from this article or parts of it. The images or other third party material in this article are included in the article's Creative Commons licence, unless indicated otherwise in a credit line to the material. If

material is not included in the article's Creative Commons licence and your intended use is not permitted by statutory regulation or exceeds the permitted use, you will need to obtain permission directly from the copyright holder. To view a copy of this licence, visit http://creativecommons.org/licenses/by-nc-nd/4.0/.

References

Abdel-Karim A, Leaper S, Skuse C, Zaragoza G, Gryta M, Gorgojo P (2021) Membrane cleaning and pretreatments in membrane distillation–a review. Chem Eng J 422:129696

Alharati A, Valour JP, Urbaniak S, Swesi Y, Fiaty K, Charcosset C (2018) Boron removal from seawater using a hybrid sorption/microfiltration process without continuous addition of resin. Chem Eng Process Proc Intensif 131:227–233. https://doi.org/10.1016/j.cep.2018.07.019

Al-Harby NF, El Batouti M, Elewa MM (2023) A comparative analysis of pervaporation and membrane distillation techniques for desalination utilising the sweeping air methodology with novel and economical pervaporation membranes. Polymers. https://doi.org/10.3390/polym15214237

Ali A, Shirazi MMA, Nthunya L, Castro-Muñoz R, Ismail N, Tavajohi N, Quist-Jensen CA (2024) Progress in module design for membrane distillation. Desalination 581:117584

Alkhudhiri A, Darwish N, Hilal N (2012) Membrane distillation: a comprehensive review. Desalination 287:2–18. https://doi.org/10.1016/j.desal.2011.08.027

Alkhudhiri A, Darwish NB, Hakami MW, Abdullah A, Alsadun A, Homod HA (2020) Boron removal by membrane distillation: a comparison study. Membranes 10(10):1–15. https://doi.org/10.3390/membranes10100263

Badini Pourazar M, Mohammadi T, Jafari Nasr MR, Bakhtiari O, Javanbakht M (2020) Preparation and characterization of poly (vinylidene fluoride)-13X zeolite mixed matrix membranes for lithium ion batteries' separator with enhanced performance. J Appl Polym Sci 137(44):49367

Boubakri A, Bouguecha SAT, Dhaouadi I, Hafiane A (2015) Effect of operating parameters on boron removal from seawater using membrane distillation process. Desalination 373:86–93. https://doi.org/10.1016/j.desal.2015.06.025

Butova VV, Vetlitsyna-Novikova KS, Pankin IA, Charykov KM, Trigub AL, Soldatov AV (2020) Microwave synthesis and phase transition in UiO-66/MIL-140A system. Microporous Mesoporous Mater. https://doi.org/10.1016/j.micromeso.2020.109998

Castro-Muñoz R (2023) A critical review on electrospun membranes containing 2D materials for seawater desalination. Desalination 555:116528

Castro-Muñoz R, Galiano F, de la Iglesia O, Fila V, Tellez C, Coronas J, Figoli A (2019a) Graphene oxide–Filled polyimide membranes in pervaporative separation of azeotropic methanol–MTBE mixtures. Sep Purif Technol 224:265–272

Castro-Muñoz R, Buera-González J, de la Iglesia O, Galiano F, Fíla V, Malankowska M, Coronas J (2019b) Towards the dehydration of ethanol using pervaporation cross-linked poly (vinyl alcohol)/graphene oxide membranes. J Membr Sci 582:423–434

Chapman PD, Oliveira T, Livingston AG, Li K (2008) Membranes for the dehydration of solvents by pervaporation. J Membr Sci 318:5–37. https://doi.org/10.1016/j.memsci.2008.02.061

Chen Z, Rana D, Matsuura T, Yang Y, Lan CQ (2014) Study on the structure and vacuum membrane distillation performance of PVDF composite membranes: I. Influence of blending. Sep Purif Technol 133:303–312. https://doi.org/10.1016/j.seppur.2014.07.015

Chen X, Chen T, Li J, Qiu M, Fu K, Cui Z, Fan Y, Drioli E (2019) Ceramic nanofiltration and membrane distillation hybrid membrane processes for the purification and recycling of boric acid from simulative radioactive waste water. J Membr Sci 579:294–301. https://doi.org/10.1016/j.memsci.2019.02.044

Drioli E, Ali A, Macedonio F (2015) Membrane distillation: recent developments and perspectives. Desalination 356:56–84

Eryildiz B, Ozbey-Unal B, Gezmis-Yavuz E, Koseoglu-Imer DY, Keskinler B, Koyuncu I (2021a) Flux-enhanced reduced graphene oxide (rGO)/PVDF nanofibrous membrane distillation membranes for the removal of boron from geothermal water. Sep Purif Technol. https://doi.org/10.1016/j.seppur.2021.119058

Eryildiz B, Yuksekdag A, Korkut S, Koyuncu İ (2021b) Performance evaluation of boron removal from wastewater containing high boron content according to operating parameters by air gap membrane distillation. Environ Technol Innov. https://doi.org/10.1016/j.eti.2021.101493

Gantenbein UL (2017) Poison and Its Dose. Toxicology in the Middle Ages and Renaissance. Elsevier, pp 1–10. https://doi.org/10.1016/B978-0-12-809554-6.00001-9

Geleta TA, Maggay IV, Chang Y, Venault A (2023) Recent advances on the fabrication of antifouling phase-inversion membranes by physical blending modification method. Membranes 13(1):58

Gontarek-Castro E, Castro-Muñoz R (2024) How to make membrane distillation greener: a review of environmentally friendly and sustainable aspects. Green Chem 26(1):164–185. https://doi.org/10.1039/D3GC03377E

Gontarek-Castro E, Castro-Muñoz R, Lieder M (2022) New insights of nanomaterials usage toward superhydrophobic membranes for water desalination via membrane distillation: a review. Crit Rev Environ Sci Technol 52(12):2104–2149

Gryta M (2005) Long-term performance of membrane distillation process. J Membr Sci 265(1–2):153–159

Gude VG (2017) Desalination and water reuse to address global water scarcity. Rev Environ Sci Biotechnol 16(4):591–609. https://doi.org/10.1007/s11157-017-9449-7

Guillerm V, Ragon F, Dan-Hardi M, Devic T, Vishnuvarthan M, Campo B, Vimont A, Clet G, Yang Q, Maurin G, Férey G, Vittadini A, Gross S, Serre C (2012) A series of isoreticular, highly stable, porous zirconium oxide based metal-organic frameworks. Angewandte Chem Int Ed 51(37):9267–9271. https://doi.org/10.1002/anie.201204806

Henrique A, Maity T, Zhao H, Brântuas PF, Rodrigues AE, Nouar F, Ghoufi A, Maurin G, Silva JAC, Serre C (2020) Hexane isomers separation on an isoreticular series of microporous Zr carboxylate metal organic frameworks. J Mater Chem A 8(34):17780–17789. https://doi.org/10.1039/d0ta05538g

Hołda AK, Vankelecom IFJ (2015) Understanding and guiding the phase inversion process for synthesis of solvent resistant nanofiltration membranes. J Appl Polym Sci. https://doi.org/10.1002/app.42130

Hong DH, Shim HS, Ha J, Moon HR (2021) MOF-on-MOF architectures: applications in separation, catalysis, and sensing. Bull Korean Chem Soc 42(7):956–969. https://doi.org/10.1002/bkcs.12335

Jia F, Li J, Wang J (2017) Recovery of boric acid from the simulated radioactive wastewater by vacuum membrane distillation crystallization. Ann Nucl Energy 110:1148–1155. https://doi.org/10.1016/j.anucene.2017.07.024

Kalaj M, Bentz KC, Ayala S, Palomba JM, Barcus KS, Katayama Y, Cohen SM (2020) MOF-polymer hybrid materials: from simple composites to tailored architectures. Chem Rev 120(16):8267–8302. https://doi.org/10.1021/acs.chemrev.9b00575

Kang GD, Cao YM (2014) Application and modification of poly(vinylidene fluoride) (PVDF) membranes—a review. J Membr Sci 463:145–165. https://doi.org/10.1016/j.memsci.2014.03.055

Khayet M, Matsuura T (2004) Pervaporation and vacuum membrane distillation processes: modeling and experiments. AIChE J 50(8):1697–1712. https://doi.org/10.1002/aic.10161

Kuznetsov YP, Kruchinina EV, Baklagina YG, Khripunov AK, Tulupova OA (2007) Deep desalination of water by evaporation through polymeric membranes. Russ J Appl Chem 80(5):790–798. https://doi.org/10.1134/S1070427207050199

Li Y, Thomas ER, Molina MH, Stewart Mann W, Walker S, Lind ML, Perreault F (2023) Desalination by membrane pervaporation: a review. Desalination 547:116223. https://doi.org/10.1016/j.desal.2022.116223

Liang W, Babarao R, D'Alessandro DM (2013) Microwave-assisted solvothermal synthesis and optical properties of tagged MIL-140A metal-organic frameworks. Inorg Chem 52(22):12878–12880. https://doi.org/10.1021/ic4024234

Liang B, Pan K, Li L, Giannelis EP, Cao B (2014) High performance hydrophilic pervaporation composite membranes for water desalination. Desalination 347:199–206. https://doi.org/10.1016/j.desal.2014.05.021

Lipnizki F, Hausmanns S, Ten PK, Field RW, Laufenberg G (1999) Organophilic pervaporation: prospects and performance. Chem Eng J 73(2):113–129

Liu G, Jin W (2021) Pervaporation membrane materials: recent trends and perspectives. J Membr Sci 636:119557. https://doi.org/10.1016/j.memsci.2021.119557

Mericq JP, Laborie S, Cabassud C (2009) Vacuum membrane distillation for an integrated seawater desalination process. Desalin Water Treat 9(1–3):287–296

Mutlu Salmanli O, Yuksekdag A, Koyuncu I (2022) Boron removal by using vacuum assisted air gap membrane distillation (VAGMD). Environ Technol Innov. https://doi.org/10.1016/j.eti.2022.102395

Mutlu-Salmanli O, Eryildiz B, Vatanpour V, Deliballi Z, Kiskan B, Koyuncu I (2023) Fabrication of novel hydrophobic electrospun nanofiber membrane using polybenzoxazine for membrane distillation application. Desalination. https://doi.org/10.1016/j.desal.2022.116203

Najid N, Kouzbour S, Ruiz-García A, Fellaou S, Gourich B, Stiriba Y (2021) Comparison analysis of different technologies for the removal of boron from seawater: a review. J Environ Chem Eng 9(2):105133. https://doi.org/10.1016/j.jece.2021.105133

Nielsen FH (2014) Update on human health effects of boron. J Trace Elements Med Biol 28:383–387. https://doi.org/10.1016/j.jtemb.2014.06.023

Nigiz FU, Karakoca B (2023) Pervaporative desalination using MIL 140A loaded polylactic acid nanocomposite membrane. Process Saf Environ Prot 169:447–457. https://doi.org/10.1016/j.psep.2022.11.015

Nofar M, Sacligil D, Carreau PJ, Kamal MR, Heuzey MC (2019) Poly (lactic acid) blends: processing, properties and applications. Int J Biol Macromol 125:307–360. https://doi.org/10.1016/j.ijbiomac.2018.12.002

Ortiz I, Urtiaga AM, Ruiz G (2001) Parallelism and differences of pervaporation and vacuum membrane distillation in the removal of VOCs from aqueous streams. In: Separation and Purification Technology. www.elsevier.com/locate/seppur

Ozbey-Unal B, Gezmis-Yavuz E, Eryildiz B, Koseoglu-Imer DY, Keskinler B, Koyuncu I (2020) Boron removal from geothermal water by nanofiber-based membrane distillation membranes with significantly improved surface hydrophobicity. J Environ Chem Eng. https://doi.org/10.1016/j.jece.2020.104113

Ozekmekci M, Unlu D, Copur M (2021) Removal of boron from industrial wastewater using PVP/PVDF blend membrane and GO/PVP/PVDF hybrid membrane by pervaporation. Korean J Chem Eng 38(9):1859–1869. https://doi.org/10.1007/s11814-021-0845-x

Prihatiningtyas I, Van der Bruggen B (2020) Nanocomposite pervaporation membrane for desalination. Chem Eng Res des 164:147–161. https://doi.org/10.1016/j.cherd.2020.10.005

Ravi J, Othman MHD, Matsuura T, Ro'il Bilad M, El-badawy TH, Aziz F, Ismail AF, Rahman MA, Jaafar J (2020) Polymeric membranes for desalination using membrane distillation: a review. Desalination. https://doi.org/10.1016/j.desal.2020.114530

Sarkar D, Sheikh AA, Batabyal K, Mandal B (2014) Boron estimation in soil, plant, and water samples using spectrophotometric methods. Commun Soil Sci Plant Anal 45(11):1538–1550. https://doi.org/10.1080/00103624.2014.904336

Segal H, Birnhack L, Nir O, Lahav O (2018) Intensification and energy minimization of seawater reverse osmosis desalination through high-pH operation: temperature dependency and second pass implications. Chem Eng Process Process Intensif 131:84–91. https://doi.org/10.1016/j.cep.2018.07.009

Si Z, Xiang J, Han D (2022) Performance analysis of a vacuum membrane distillation system coupled with heat pump for sulfuric acid solution treatment. Chem Eng Process Process Intensif. https://doi.org/10.1016/j.cep.2021.108734

Smitha B, Suhanya D, Sridhar S, Ramakrishna M (2004) Separation of organic-organic mixtures by pervaporation—a review. J Membr Sci 241:1–21. https://doi.org/10.1016/j.memsci.2004.03.042

Tan B, Selengil U, Bektas TE (2021) Boron rejection from aqueous solution and wastewater by direct contact membrane distillation. Environ Res Technol 4(1):73–82

Tan B, Yildiz S, Angın D, Bektaş TE, Selengil U (2024) Boron removal from wastewater by direct contact membrane distillation system using two-level factorial design. J Appl Water Eng Res 12(1):39–49. https://doi.org/10.1080/23249676.2023.2198734

Tooma MA, Najim TS, Alsalhy QF, Marino T, Criscuoli A, Giorno L, Figoli A (2015) Modification of polyvinyl chloride (PVC) membrane for vacuum membrane distillation (VMD) application. Desalination 373:58–70. https://doi.org/10.1016/j.desal.2015.07.008

Ünügül T, Nigiz FU (2022) Evaluation of halloysite nanotube-loaded chitosan-based nanocomposite membranes for water desalination by pervaporation. Water Air Soil Pollut. https://doi.org/10.1007/s11270-022-05505-z

Van De Voorde B, Damasceno Borges D, Vermoortele F, Wouters R, Bozbiyik B, Denayer J, Taulelle F, Martineau C, Serre C, Maurin G, De Vos D (2015) Isolation of renewable phenolics by adsorption on ultrastable hydrophobic MIL-140 metal-organic frameworks. Chemsuschem 8(18):3159–3166. https://doi.org/10.1002/cssc.201500281

Vatanpour V, Yuksekdag A, Ağtaş M, Mehrabi M, Salehi E, Castro-Muñoz R, Koyuncu I (2023) Zeolitic imidazolate framework (ZIF-8) modified cellulose acetate NF membranes for potential water treatment application. Carbohyd Polym 299:120230

Vatanpour V, Ardic R, Esenli B, Eryildiz-Yesir B, Pazoki PY, Jarahiyan A, Koyuncu I (2024) Defected Ag/Cu-MOF as a modifier of polyethersulfone membranes for enhancing permeability, antifouling properties and heavy metal and dye pollutant removal. Separ Purif Technol 345:127336

Wang Q, Li N, Bolto B, Hoang M, Xie Z (2016) Desalination by pervaporation: a review. Desalination 387:46–60. https://doi.org/10.1016/j.desal.2016.02.036

Wen X, Li F, Zhao X (2016) Removal of nuclides and boron from highly saline radioactive wastewater by direct contact membrane distillation. Desalination 394:101–107. https://doi.org/10.1016/j.desal.2016.05.001

Woo YC, Kim Y, Yao M, Tijing LD, Choi JS, Lee S, Shon HK (2018) Hierarchical composite membranes with robust omniphobic surface using layer-by-layer assembly technique. Environ Sci Technol 52(4):2186–2196

Wu T, Prasetya N, Li K (2020) Recent advances in aluminium-based metal-organic frameworks (MOF) and its membrane applications. J Membr Sci. https://doi.org/10.1016/j.memsci.2020.118493

Xue Y, Shen M, Zheng Y, Tao W, Han Y, Li W, Wang H (2020) One-pot scalable fabrication of an oligomeric phosphoramide towards high-performance flame retardant polylactic acid with a submicron-grained structure. Compos Part B Eng 183:107695

Yadav A, Labhasetwar PK, Shahi VK (2021a) Fabrication and optimization of tunable pore size poly(ethylene glycol) modified poly(vinylidene-co-hexafluoropropylene) membranes in vacuum membrane distillation for desalination. Separ Purif Technol. https://doi.org/10.1016/j.seppur.2021.118840

Yadav A, Yadav P, Labhasetwar PK, Shahi VK (2021b) CNT functionalized ZIF-8 impregnated poly(vinylidene fluoride-co-hexafluoropropylene) mixed matrix membranes for antibiotics removal from pharmaceutical industry wastewater by vacuum membrane distillation. J Environ Chem Eng. https://doi.org/10.1016/j.jece.2021.106560

Yahaya NZS, Paiman SH, Abdullah N, Muammar Mahpoz N, Raffi AA, Rahman MA, Abas KH, Aziz AA, Othman MHD, Jaafar J (2020) Synthesis and characterizations of MIL-140B-Al2O3/YSZ ceramic membrane using solvothermal method for seawater desalination. J Aust Ceramic Soc 56(1):291–300. https://doi.org/10.1007/s41779-019-00435-2

Yapici D (2011) Recycle Study Of Ion Exchange-Membrane Filtration Hybrid Process For Boron Removal From Geothermal Water. Ege University Graduate School Of Natural And Applied Sciences (Master Thesis)

Zhou R, Rana D, Matsuura T, Lan CQ (2019) Effects of multi-walled carbon nanotubes (MWCNTs) and integrated MWCNTs/SiO2 nano-additives on PVDF polymeric membranes for vacuum membrane distillation. Sep Purif Technol 217:154–163. https://doi.org/10.1016/j.seppur.2019.02.013

Publisher's Note Springer Nature remains neutral with regard to jurisdictional claims in published maps and institutional affiliations.